

## **H<sub>2</sub>O Masers in the Galactic Plane. II\*** **Longitudes 260° to 326°**

*J. L. Caswell, R. A. Batchelor, J. R. Forster and K. J. Wellington*

Division of Radiophysics, CSIRO, P.O. Box 76, Epping, N.S.W. 2121, Australia.

### *Abstract*

We present details of 53 H<sub>2</sub>O masers located in the galactic plane between longitudes 260° and 326°. Twenty-one of these are new ones found at the sites of recently discovered OH masers. The properties of the individual masers are discussed, in particular the variability of sources known for several years and the high velocity emission exhibited by some masers. The association of H<sub>2</sub>O and OH masers has been investigated and out of 36 OH masers in this region of sky, a remarkably high number (34) have nearby H<sub>2</sub>O masers.

### **1. Introduction**

In earlier studies we have investigated the occurrence of maser emission from H<sub>2</sub>O (rest frequency 22·23508 GHz) near mainline (1665 and 1667 MHz) OH masers. Longitude ranges 340° to the galactic centre (Caswell *et al.* 1983*a*) and 3° to 60° (Caswell *et al.* 1983*b*) are now supplemented by the present study for longitudes 260° to 326°, a region with 36 OH masers (35 listed by Caswell and Haynes 1987*a*, plus OH 323·74-0·27). In addition to searching at the positions of all the OH masers, we present further measurements of H<sub>2</sub>O masers discovered in this region with the Itapetinga telescope, many of them with no known OH counterpart.

### **2. Observations**

The present measurements were made chiefly in the periods 1981 December and 1982 April with a maser receiver on the Parkes 64-m radio telescope. The beamwidth to half-power was 100'' arc and the system temperature ~60 K. All measurements were made with a linearly polarised feed with the E-plane aligned vertically; 1 K (antenna temperature after correction for atmospheric absorption) corresponds to an (unpolarised) point source flux density of 9 Jy. Our observing technique was identical to that described by Caswell *et al.* (1983*a*, 1983*b*). The 1024-channel correlator covered 320 km s<sup>-1</sup> (24 MHz), with velocity resolution 0·53 km s<sup>-1</sup> over the central 135 km s<sup>-1</sup> band. In 5-minute integrations the 3σ detection level sensitivity was between 1 and 2 Jy, depending on the weather conditions and telescope elevation angle. A grid of observations around each source yielded positions with r.m.s. errors of ~12'' arc in each coordinate. For

\* Part I, *Aust. J. Phys.*, 1983, 36, 401-15.

many of the sources we have subsequently made additional measurements and the averaged position quoted has a correspondingly smaller error.

### 3. Results

Table 1 summarises our Parkes H<sub>2</sub>O results in this region of the galactic plane; 53 H<sub>2</sub>O masers are listed together with two null results at the positions of OH masers. Columns 1–3 give the H<sub>2</sub>O positions and column 4 the radial velocity of the strongest emission. Column 5 lists the width of this strongest feature, or refers to the appropriate figure. Column 6 lists the maximum intensity; where enclosed in parentheses it refers to other observations cited in column 7. Column 7 also draws attention to notes in the text and the presence of high-velocity emission. Any nearby OH maser that seems likely to be associated with the H<sub>2</sub>O maser is listed in column 8. Spectra for most of the sources are shown in Figs 1–5; the full 320 km s<sup>-1</sup> range is not shown unless the presence of high-velocity emission requires this. Where no figure is cited in column 5 of Table 1, a spectrum can generally be found in the reference of column 7. Note that for previously catalogued sources we have used our new position measurements to assign preferred names as used in Table 1, figures and text; these may differ slightly from the earlier designations but should cause no ambiguity. Where there are several very nearby but separate maser sites, we have listed them as separate sources and commented on the association in the following notes. The notes also give some specific details on variability and high-velocity emission. Remarks on accompanying OH emission are based on the data of Caswell and Haynes (1987*a*), and remarks on associated HII regions are based on data of Caswell and Haynes (1987*b*).

#### *Notes on Individual H<sub>2</sub>O Masers*

*H<sub>2</sub>O 264.29+1.46 and H<sub>2</sub>O 264.29+1.47 (Fig. 1).* Emission first reported by Braz and Scalise (1982); our measurements show that two sources are present, 26'' arc apart. The maser at  $v = +5.5$  km s<sup>-1</sup> increased in intensity by a factor of 5 and the other maser decreased by a factor of 2 between 1979 and 1981.

*H<sub>2</sub>O 267.94-1.06 (Fig. 1).* Earlier measurements (Batchelor *et al.* 1980) showed the central feature near  $v = 0$  km s<sup>-1</sup> to be weaker than other features at -18, +18 and +37 km s<sup>-1</sup>. The central feature is now the strongest.

*H<sub>2</sub>O 269.15-1.13 (Fig. 1).* There is an associated HII region with  $v = +15$  km s<sup>-1</sup> (kinematic distance 3.6 kpc) corresponding to the brighter H<sub>2</sub>O feature.

*H<sub>2</sub>O 284.35-0.42.* This is an intense well-studied maser. Nearby, a weak source designated H<sub>2</sub>O 284.3-0.3 was reported by Kaufmann *et al.* (1977) but not detected in subsequent searches. We have not listed this weak source since no precise position was ever measured and it is possible that the Kaufmann *et al.* result refers to the much stronger maser, H<sub>2</sub>O 284.35-0.42, detected at the edge of the beam.

*H<sub>2</sub>O 285·26-0·05.* See Batchelor *et al.* (1982) for a spectrum and a discussion of the high-velocity features.

*H<sub>2</sub>O 291·27-0·71, H<sub>2</sub>O 291·28-0·71, and H<sub>2</sub>O 291·27-0·72 (Fig. 1).* The three centres of emission are separated by only  $\sim 50''$  arc and the second and third features may be regarded as high-velocity features associated with the first one. At an estimated kinematic distance of 3·6 kpc (Caswell and Haynes 1987*b*),  $50''$  arc corresponds to 0·9 pc. *H<sub>2</sub>O 291·28-0·71*, the highest velocity ( $v = -126 \text{ km s}^{-1}$ ) feature, is stronger than emission at the systemic (low) velocity; this was also true at earlier epochs (Goss *et al.* 1977; Batchelor *et al.* 1980) and now it is stronger than ever before. The intermediate velocity ( $v = -88 \text{ km s}^{-1}$ ) feature *H<sub>2</sub>O 291·27-0·72* is new and quite intense. The spectrum shown in Fig. 1 is at an average position (R.A.  $11^{\text{h}}04^{\text{m}}41\cdot9^{\text{s}}$ , Dec  $-61^{\circ}20'02\cdot38''$ ) so as to show all three features; at this offset position the measured intensities are lower than the true values and have been corrected in Table 1 by factors of 1·24 (*H<sub>2</sub>O 291·28-0·71*), 1·15 (*H<sub>2</sub>O 291·27-0·72*) and 1·40 (*H<sub>2</sub>O 291·27-0·71*).

*H<sub>2</sub>O 291·58-0·43, H<sub>2</sub>O 291·61-0·53, H<sub>2</sub>O 291·63-0·53, H<sub>2</sub>O 291·64-0·55 and H<sub>2</sub>O 291·65-0·60 (Fig. 2).* The first of these sources has been known for many years and a further source was noted by Braz and Scalise (1982). The whole remarkable cluster of sources was discussed by Batchelor *et al.* (1982) and at several positions more than one source is contained in the beam. In each spectrum shown in Fig. 2, emission from adjacent sources has been shaded. Some sources now show high-velocity features.

*H<sub>2</sub>O 300·50-0·18 (Fig. 3).* There is a corresponding associated OH maser (Caswell and Haynes 1987*a*) and also a weak HII region in this direction with  $v = +26 \text{ km s}^{-1}$  (Caswell and Haynes 1987*b*) corresponding to a kinematic distance of 12·5 kpc (and galactocentric radius 11·4 kpc). The major *H<sub>2</sub>O* peak is approximately at this velocity and the other features, extending from  $-53$  to  $+50 \text{ km s}^{-1}$ , presumably represent high-velocity ejecta. The multiplicity of high-velocity features make this an outstanding candidate for studies at higher resolution with a long-baseline interferometer.

*H<sub>2</sub>O 300·97+1·14 (Fig. 3).* The HII region in this direction has a velocity of  $-47 \text{ km s}^{-1}$  (Caswell and Haynes 1987*b*), and the *H<sub>2</sub>O* emission is also strongest near this velocity, which we take to be the systemic velocity (surprisingly the OH is centred near  $-38 \text{ km s}^{-1}$ ). *H<sub>2</sub>O* high-velocity emission is present at velocities both higher and lower than the systemic velocity.

*H<sub>2</sub>O 301·14-0·23 (Fig. 3).* The corresponding HII region is weak with no recombination line measured as yet but the associated OH maser has its strongest feature at  $v \sim -40 \text{ km s}^{-1}$  (Caswell and Haynes 1987*a*) and we take this to be most likely the systemic velocity. The *H<sub>2</sub>O* emission at  $v = -40 \text{ km s}^{-1}$  has weakened since its discovery (Braz and Scalise 1982) and the emission at  $v = -30 \text{ km s}^{-1}$  has flared by a factor of  $\sim 5$  making it currently the strongest feature. High-velocity features are present at the more negative velocities  $v = -60$  and  $-73 \text{ km s}^{-1}$ . The OH maser emission is of considerable interest because it, too, shows high-velocity features at negative velocities,  $-50$  and  $-64 \text{ km s}^{-1}$  (Caswell and Haynes 1987*a*).

Table 1. H<sub>2</sub>O masers and associated OH masers in the galactic longitude range 260° to 326°

H <sub>2</sub> O maser gal. coords. (l', b')	RA (1950) h m s	Dec (1950) ° ' "	Radial velocity (km s <sup>-1</sup> )	Velocity width (kms <sup>-1</sup> )	Peak Intensity (Jy)	H <sub>2</sub> O references <sup>a</sup> and remarks	OH maser gal. coords. (l', b')
264.29+1.46	08 54 36.2	-42 54 12	+10.5	see Fig.1	36	BS82; text	-
264.29+1.47	08 54 38.5	-42 54 06	+5.5	see Fig.1	171	BS82; text	-
265.14+1.45	08 57 35.9	-43 33 30	+9.5	see Fig.1	10.7	BS82	-
267.94-1.06	08 57 21.9	-47 18 59	-1	see Fig.1	122	B+80; text; high vel.	-
269.15-1.13	09 01 53.0	-48 16 07	+16.5	see Fig.1	49	SB80; text	-
270.26+0.84	09 14 56.3	-47 43 34	+8	see Fig.1	545	SB80	-
284.35-0.42	10 22 21.6	-57 37 29	+7	~4	(340)	B+80; text	-
285.26-0.05	10 29 37.0	-57 46 49	+8	see text	1875	B+82; text; high vel.	OH 285.26-0.05
287.37-0.62	10 41 34.9	-59 18 29	-17.5	see Fig.1	42	SB80	-
291.27-0.71	11 09 44.9	-61 02 01	-32	see Fig.1	200	B+80; text; high vel.	-
291.28-0.71	11 09 48.0	-61 02 36	-126	see Fig.1	1300	B+80; text; high vel.	-
291.27-0.72	11 09 41.5	-61 02 29	-88	see Fig.1	270	B+80; text; high vel.	-
291.58-0.43	11 12 56.8	-60 53 19	+13	see Fig.2	790	B+82; text	OH 291.57-0.43
291.61-0.53	11 12 54.5	-60 59 36	+12.2	see Fig.2	70	B+82; text; high vel.	OH 291.61-0.53
291.63-0.53	11 13 01.5	-60 59 48	+23	see Fig.2	16.5	B+82; text	-
291.64-0.55	11 13 04.8	-61 01 07	+1.2	see Fig.2	62	B+82; text	-
291.65-0.60	11 13 01.4	-61 04 07	+14	see Fig.2	31	B+82; text	-
297.66-0.97	12 01 33.6	-63 04 53	+24	see Fig.2	72	-	OH 297.66-0.98
298.22-0.34	12 07 19.0	-62 32 56	+28.5	see Fig.2	9	BS82	-
299.01+0.13	12 14 42.1	-62 12 19	+26	see Fig.2	60	BS82	OH 299.02+0.13
300.50-0.18	12 27 14.0	-62 40 19	+30	see Fig.3	530	B+80; text; high vel.	OH 300.51-0.18
300.97+1.14	12 32 00.8	-61 23 30	-47.5	see Fig.3	47	BS82; text; high vel.	OH 300.97+1.15
301.14-0.23	12 32 41.2	-62 46 07	-29.5	see Fig.3	250	text;	OH 301.14-0.23
305.20+0.01	13 08 04.7	-62 30 33	-32.5	see Fig.3	13.6	-	OH 305.21+0.03
305.21+0.21	13 08 01.9	-62 18 44	-41	~2	(150)	B+80	OH 305.20+0.21

305.36+0.15	13 09 22.6	-62 21 27	-37	~2	(40; 70)	B+80	OH 305.36+0.15
305.37+0.21	13 09 23.8	-62 17 45	-37	~4	(60; 70)	B+80;	-
305.36+0.20	13 09 19.7	-62 18 34	-90	~4	(>25)	B+80;	high vel.
305.80-0.24	13 13 26.7	-62 42 43	-33.8	see Fig.3	2000	text	OH 305.81-0.24
Non-detection at OH position				-	<2	-	OH 306.32-0.36
308.92+0.12	13 39 33.2	-61 53 59	-59.5	see Fig.3	6.8	BS82; text	OH 308.92+0.12
309.38-0.14	13 43 53.3	-62 03 27	-70.5	see Fig.3	39.5	-	OH 309.39-0.13
309.93+0.48	13 47 14.7	-61 20 25	-70.5	see text	4.5	K+77; text	OH 309.92+0.48
310.06-3.04	13 55 45.9	-64 43 08	+11	see Fig.4	13	text	OH 310.06-3.02
311.64-0.38	14 02 59.3	-61 44 06	+33	see Fig.4	405	text;	OH 311.64-0.38
311.95+0.14	14 04 12.4	-61 09 05	-41.3	see Fig.4	38	BS82; text	OH 311.94+0.14
312.60+0.04	14 09 35.3	-61 03 20	-63	see Fig.4	3.7	text	OH 312.60+0.05
313.47+0.19	14 15 59.1	-60 38 12	-4	see Fig.4	10.7	-	OH 313.47+0.19
316.41-0.31	14 39 35.0	-60 00 22	-12	see Fig.4	16.4	-	OH 316.40-0.30
316.64-0.09	14 40 29.1	-59 42 46	-18	see Fig.4	25	text;	OH 316.64-0.08
316.76-0.01	14 41 07.8	-59 35 33	-39	~2	(40; 25)	B+80	OH 316.76-0.02
316.81-0.06	14 41 36.3	-59 36 51	-46	~3	(290; 280)	B+80	OH 316.81-0.07
318.05+0.09	14 49 52.9	-58 56 47	-49	see Fig.4	620	text	OH 318.05+0.08
318.94-0.20	14 57 01.5	-58 47 14	-37.4	see Fig.5	8.0	text;	OH 318.95-0.20
Non-detection at OH position				-	<2	-	OH 319.39-0.02
319.83-0.20	15 03 00.4	-58 21 30	-5	see Fig.5	5.8	text	OH 319.83-0.21
320.23-0.29	15 05 59.6	-58 14 18	-54	see Fig.5	46.4	text;	OH 320.23-0.28
320.25-0.31	15 06 13.3	-58 14 49	-156	see Fig.5	371	text;	OH 320.23-0.28
320.28-0.31	15 06 25.7	-58 14 02	-65.8	see text	~12	text;	OH 320.23-0.28
321.15-0.53	15 12 52.7	-57 58 50	-64	see Fig.5	18.3	-	OH 321.14-0.53
322.17+0.62	15 14 50.2	-56 27 51	-52	see Fig.5	36.5	BS82; text	OH 322.16+0.63
323.46-0.09	15 25 27.8	-56 21 24	-67.5	see Fig.5	11.0	-	OH 323.46-0.08
323.74-0.27	15 27 52.4	-56 20 48	-51	~1	(480)	text;	OH 323.74-0.25
324.20+0.12	15 29 00.5	-55 45 09	-93	~1	(40)	B+80	OH 324.20+0.12
324.72+0.34	15 31 06.7	-55 17 28	-59	see Fig.5	138	text	OH 324.70+0.33

References: BS82, Braz and Scalise 1982; SB80, Scalise and Braz 1980; B+80, Batchelor et al. 1980  
 B+82, Batchelor et al. 1982; K+77, Kaufmann et al. 1977.

$H_2O\ 305.37+0.21$  and  $H_2O\ 305.36+0.20$ . Emission at  $v \sim -33\text{ km s}^{-1}$  most likely corresponds to the systemic velocity. Higher velocity emission (with intensity comparable with the main feature) occurs near  $v \sim -100\text{ km s}^{-1}$ , displaced  $\sim 50''$  arc from  $H_2O\ 305.37+0.21$  and listed as the separate source  $H_2O\ 305.36+0.20$ ; at a distance of 8 kpc, the (preferred) far kinematic distance,  $50''\text{ arc} = 1.9\text{ pc}$ .

$H_2O\ 305.80-0.24$  (Fig. 3). This is the strongest of our new masers. It coincides with an OH maser and lies amidst diffuse continuum emission with no compact counterpart detected as yet. Corresponding to its centre velocity of  $-30\text{ km s}^{-1}$ , the kinematic distance alternatives are 2.4 and 9.3 kpc; the larger of these is slightly preferred on the basis of earlier arguments concerning the probably related HII region complex (Caswell *et al.* 1975). At 9.3 kpc, the  $H_2O$  maser would be one of the most luminous in our galaxy.

$H_2O\ 308.92+0.12$  (Fig. 3). A weak source reported by Braz and Scalise (1982) and confirmed by our observations.

$H_2O\ 309.93+0.48$ . A weak source reported by Kaufmann *et al.* (1977) and now confirmed; still very weak with large ( $>30\text{ arcsec}$ ) position uncertainty, and too weak to define linewidth.

$H_2O\ 310.06-3.04$  (Fig. 4). The OH and IR data suggest that this is a late-type star, somewhat unusual because it is on the 1665 MHz transition that the OH maser is both strongest and shows the largest velocity spread (from  $-13$  to  $+8\text{ km s}^{-1}$ ). The quite weak  $H_2O$  maser is brightest at  $\sim +10\text{ km s}^{-1}$  and its characteristics are generally compatible with a late-type star interpretation; however, the wings extend to  $+20\text{ km s}^{-1}$ , well outside the range of OH emission and therefore anomalous amongst late-type stars.

$H_2O\ 311.64-0.38$  (Fig. 4). The mean velocity of this  $H_2O$  maser,  $v \sim +33\text{ km s}^{-1}$ , is in good agreement with the OH emission, and is indicative of a large distance, outside the solar circle in the Carina arm of the galaxy. The emission is strong over an unusually large continuous velocity range of  $\sim 60\text{ km s}^{-1}$ .

$H_2O\ 311.95+0.14$  (Fig. 4). Our observations show the main feature at the same velocity as in the discovery measurements of Braz and Scalise (1982).

$H_2O\ 312.60+0.04$  (Fig. 4). The weakest of our new discoveries.

$H_2O\ 316.64-0.09$  (Fig. 4). An earlier null result in this direction (upper limit 8 Jy—Caswell *et al.* 1977) suggests an intensity increase has now occurred of at least a factor of three. High-velocity emission is also now present.

$H_2O\ 318.05+0.09$  (Fig. 4). Strong emission with many blended features over a velocity range of  $20\text{ km s}^{-1}$ .

$H_2O\ 318.94-0.20$  (Fig. 5). A blend of several lines occurs between  $v = -28$  and  $-40\text{ km s}^{-1}$ , and emission almost as strong is centred at  $v = -65\text{ km s}^{-1}$ . The corresponding OH maser and nearby HII region have mean velocities of

---

**Figs 1–5.** Spectra of  $H_2O$  masers. Source names and observing dates are shown within each frame. The velocity resolution is  $0.53\text{ km s}^{-1}$  (40 kHz). The velocity coverage of each spectrum was  $320\text{ km s}^{-1}$  but the outer regions where no emission was found are not shown.

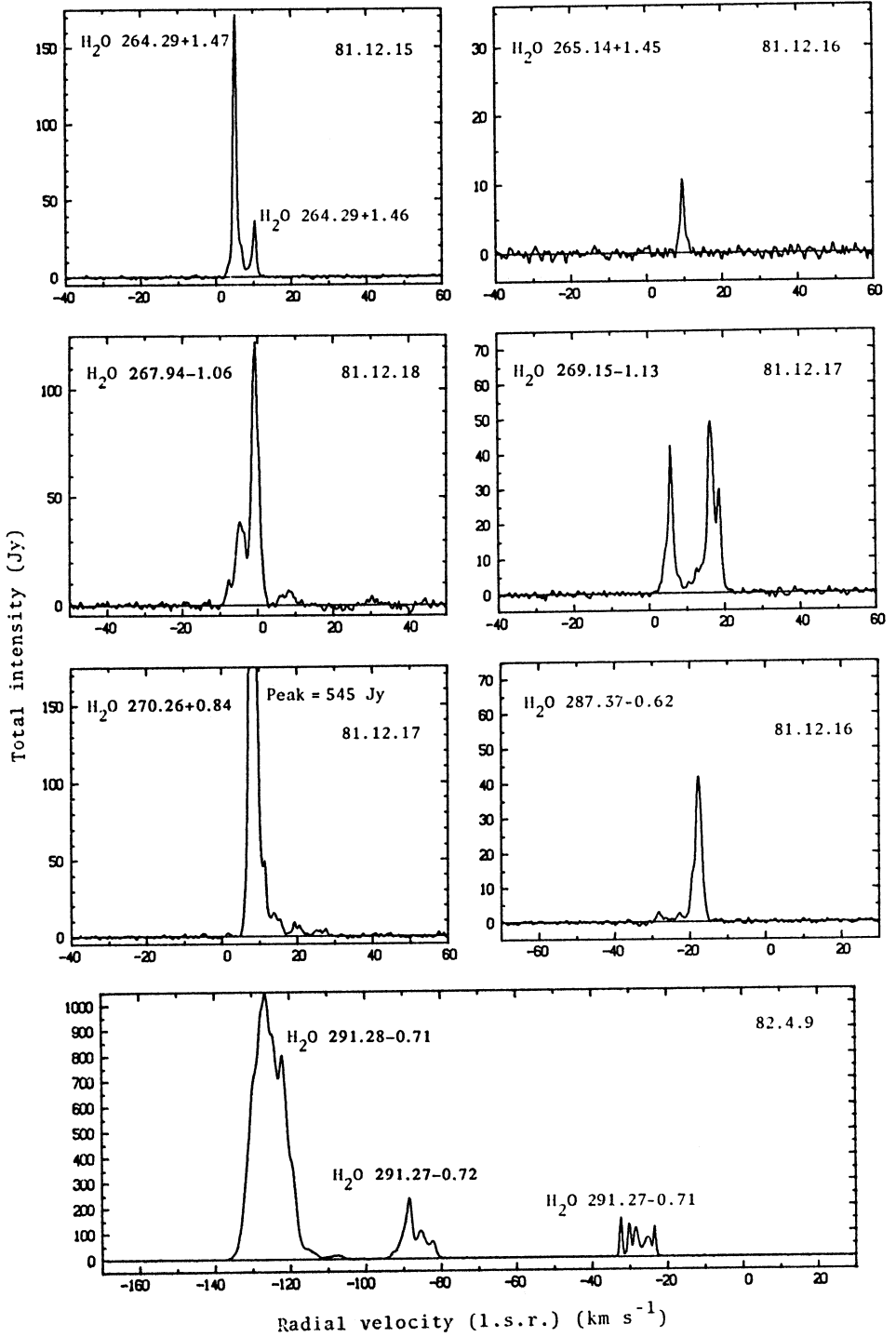


Fig. 1

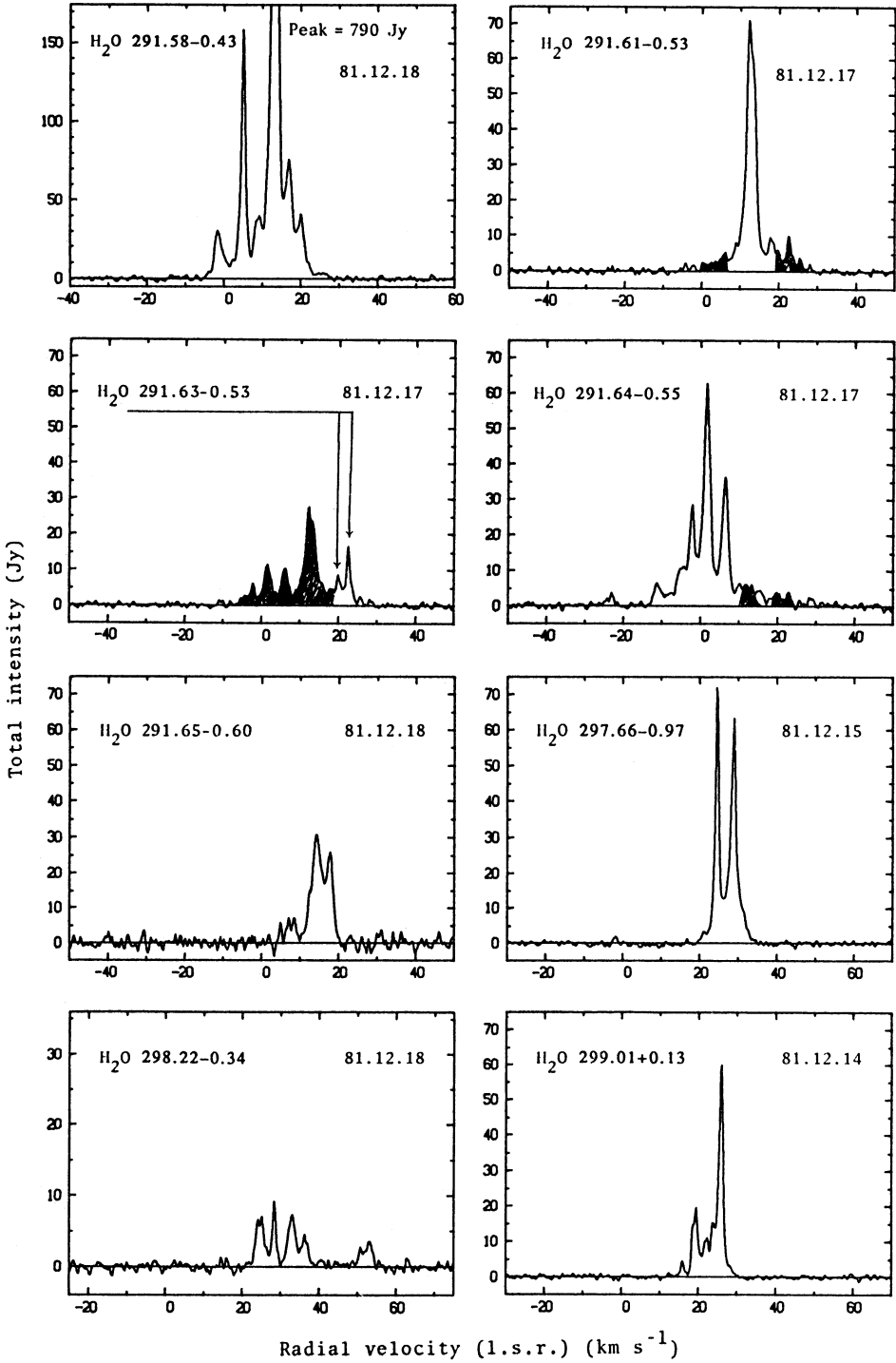


Fig. 2

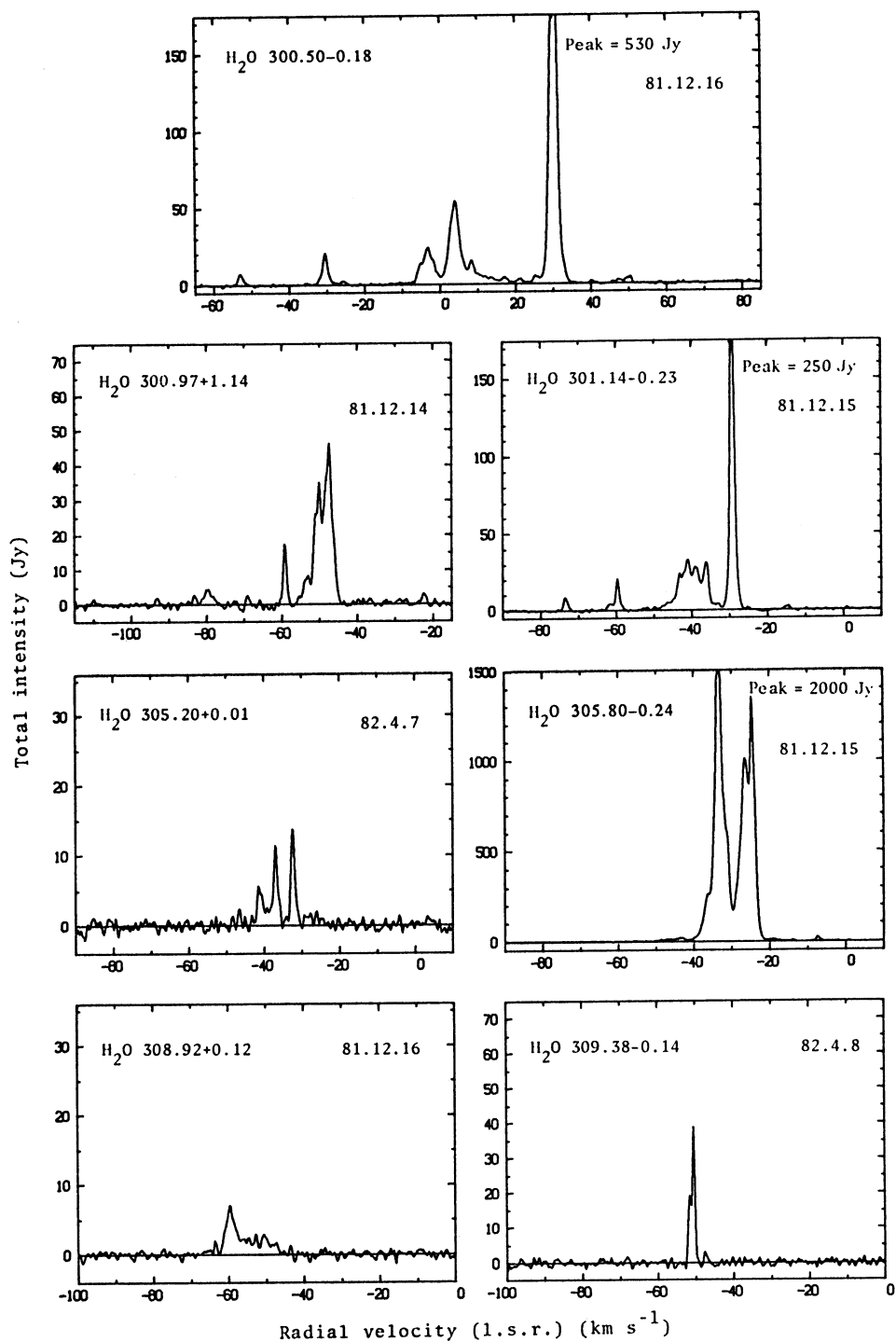


Fig. 3

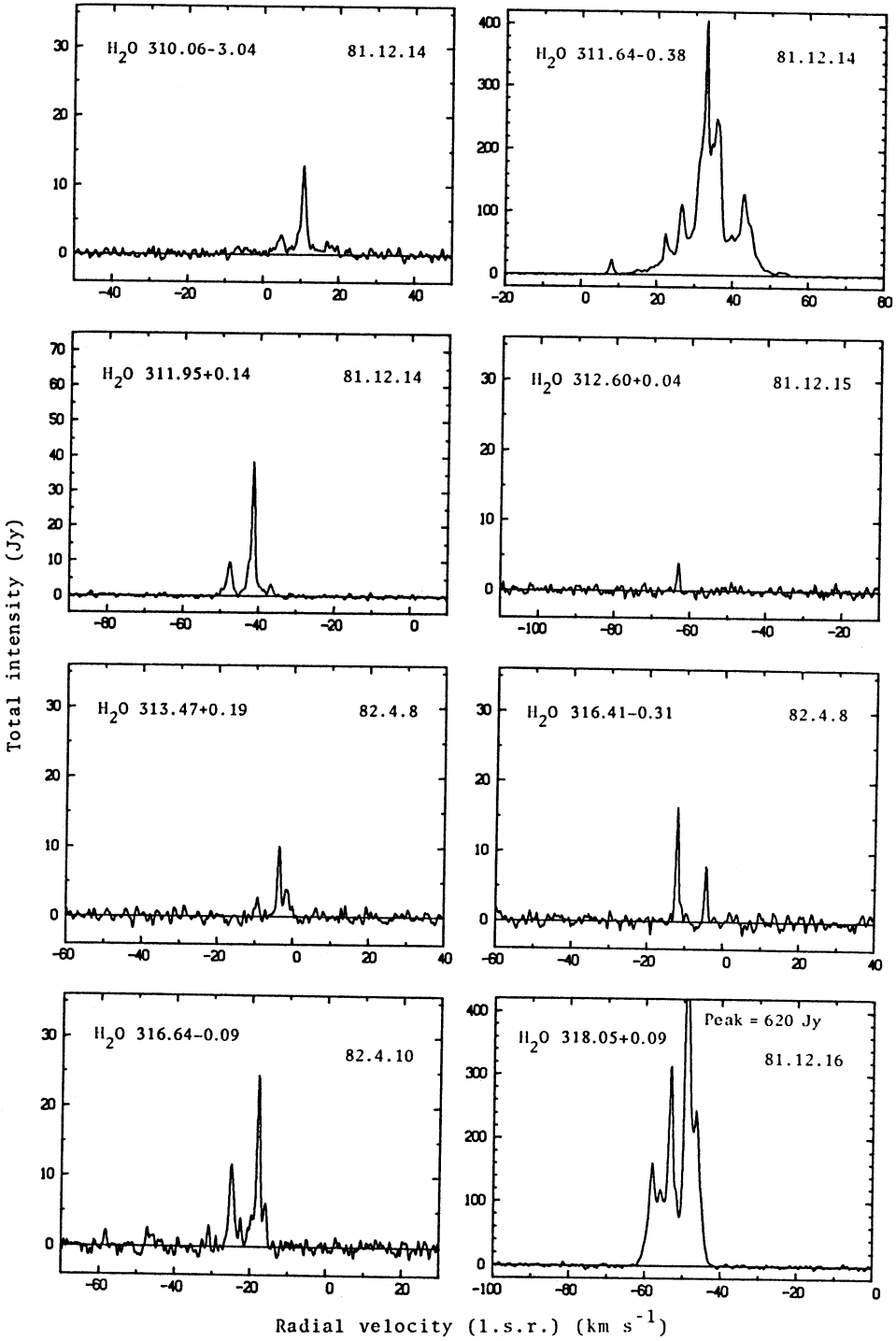


Fig. 4

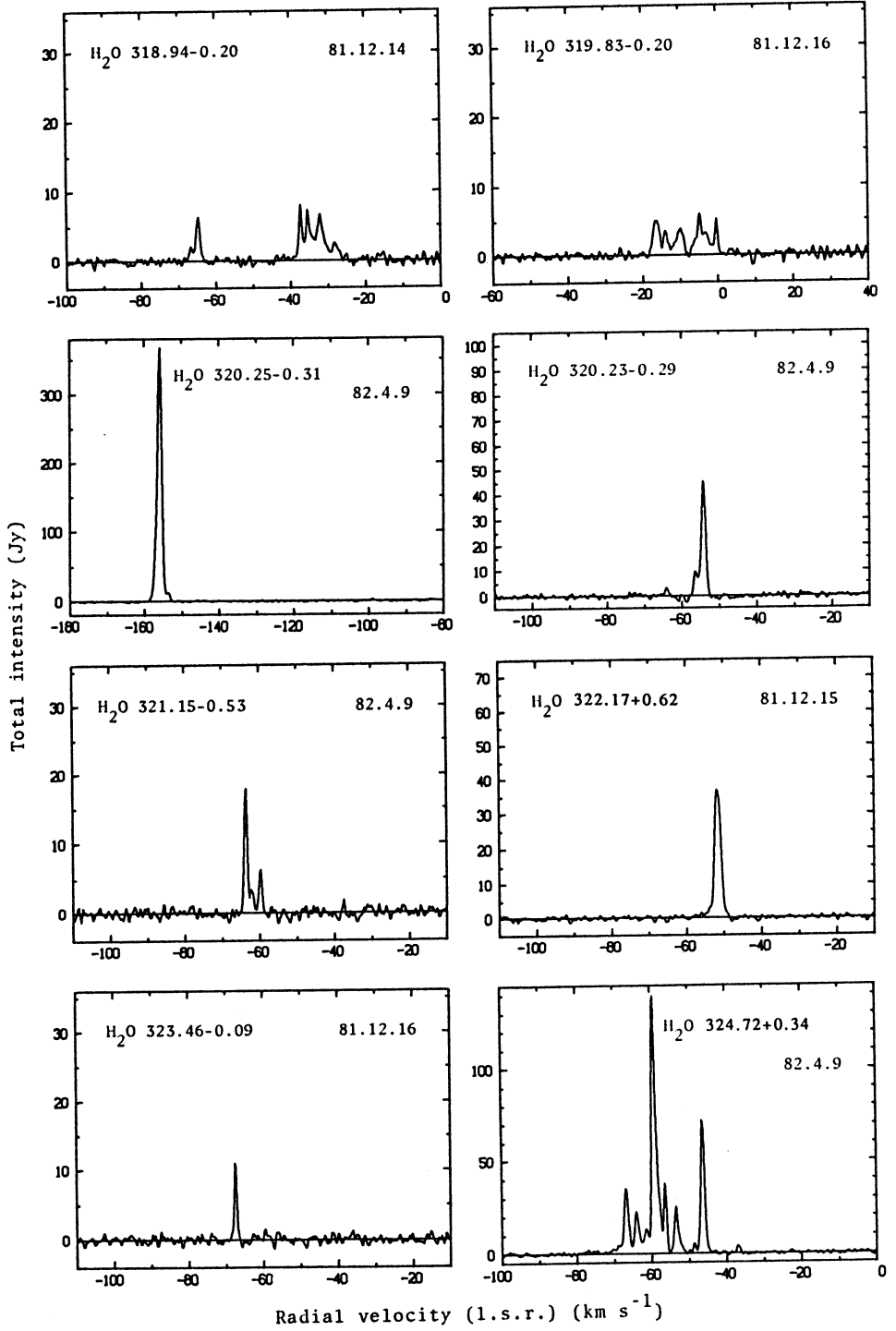


Fig. 5

$-36$  and  $-29$   $\text{km s}^{-1}$ . Probably the systemic velocity is  $\sim -30$   $\text{km s}^{-1}$ , and the  $-65$   $\text{km s}^{-1}$  emission is of the high-velocity variety.

$H_2O\ 319.83-0.20$  (Fig. 5). A weak new maser with quite large velocity spread of  $\sim 20$   $\text{km s}^{-1}$ .

$H_2O\ 320.23-0.29$ ,  $H_2O\ 320.25-0.31$  (Fig. 5), and  $H_2O\ 320.28-0.31$ . Scalise and Braz (1980) discovered the first of these sources, with velocity near  $-60$   $\text{km s}^{-1}$ . The second source has a grossly different velocity of  $v = -156$   $\text{km s}^{-1}$  and we suggest that it may represent high-velocity ejecta which is much stronger than emission at the systemic velocity. If it has been ejected from the first source, the spatial separation of  $113''$  arc is surprisingly large, corresponding to  $2.7$  pc at the likely kinematic (near) distance of  $5$  kpc. Note that ejecta at a speed of  $100$   $\text{km s}^{-1}$  will travel  $2.7$  pc in  $\sim 3 \times 10^4$  years. The situation is thus similar to (but even more extreme than) that of  $H_2O\ 291.27-0.71$  and its neighbours where, again, the highest velocity feature is the strongest and the separation is  $\sim 1$  pc. Emission from  $H_2O\ 320.28-0.31$  (not shown) is weak and displaced even further from the first source although at a similar velocity; it might be the second member of a cluster of sources rather than representing ejecta.

$H_2O\ 322.17+0.62$  (Fig. 5). First reported by Braz and Scalise (1982) and confirmed, with similar velocity and intensity, by our Parkes observations.

$H_2O\ 323.74-0.27$ . A strong  $H_2O$  maser which we discovered in June 1988; its inclusion makes Table 1 an up-to-date listing of currently known sources. The corresponding OH maser was reported by Cohen *et al.* (1988) and a very strong methanol maser on the  $12.2$  GHz transition is also present (Kemball *et al.* 1988; Norris *et al.* 1988; McCutcheon *et al.* 1988).

$H_2O\ 324.72+0.34$  (Fig. 5). The  $H_2O$  spectrum is best described as a forest of blended lines with at least eight distinct features spread over  $\sim 20$   $\text{km s}^{-1}$ .

#### 4. Discussion

##### (a) Variability

Some of the more dramatic instances of variability are remarked on in the notes but a detailed discussion is deferred until a current monitoring program has been completed.

##### (b) High-velocity Emission

Sources showing high-velocity emission are readily identified from the table, figures, and notes. In the present sample they constitute about 30% of the total. Three sources deserve discussion as a special class:  $H_2O\ 291.27-0.71$  (and its high-velocity companions),  $H_2O\ 305.37+0.21$  with  $H_2O\ 305.36+0.20$ , and  $H_2O\ 320.23-0.29$  (and its high-velocity companions). In each case the systemic velocity is quite well determined, defined by a loosely associated HII region (as well as an OH maser for the latter two). The remarkable aspect is that the high-velocity emission is either much stronger than (in the first and last examples) or at least comparable with the emission near the systemic velocity. Furthermore, the angular separation of the features is large,  $\sim 1$  arcmin, corresponding to separations of more than a parsec. In all respects the sources resemble  $H_2O\ 351.24+0.66$  and perhaps  $H_2O\ 12.2-0.1$

(see Caswell *et al.* 1983*a*; Goss *et al.* 1977; Rodriguez *et al.* 1980). All the sources in this category deserve a much more detailed study of not only the H<sub>2</sub>O emission (to ascertain whether the motion is a general expansion or a directed bi-polar flow), but also other molecules such as CO and NH<sub>3</sub> to search for further evidence of outflow and perhaps a massive rotating disk whose axis might determine a flow axis.

### (c) Association with OH Masers

Of the 36 OH masers in the region of sky studied here, 34 have nearby H<sub>2</sub>O masers. This proportion is remarkably high, somewhat exceeding the fraction in the other regions we have studied (Caswell *et al.* 1983*a*, 1983*b*). However, it is compatible with the earlier statistics and reinforces our suggestion that in any star formation region able to sustain OH masers, there are necessarily physical conditions nearby that are conducive to the excitation of H<sub>2</sub>O masers. This would be consistent with high H<sub>2</sub>O densities being a prerequisite for 1665 MHz OH maser emission as is assumed in some proposed OH pumping schemes (e.g. Kylafis and Norman 1989). The details of the associations discovered here must await observations with higher angular resolution and greater positional accuracy—similar to the investigations already begun on 70 more northerly sources by Forster and Caswell (1987, 1989).

### Acknowledgments

We are grateful to R. F. Haynes, R. A. Duncan and W. H. McCutcheon, participants in our current monitoring program, for assistance in obtaining some of the improved position data.

### References

- Batchelor, R. A., Caswell, J. L., Goss, W. M., Haynes, R. F., Knowles, S. H., and Wellington, K. J. (1980). *Aust. J. Phys.* **33**, 139.
- Batchelor, R. A., Caswell, J. L., Forster, J. R., and Wellington, K. J. (1982). *Proc. Astron. Soc. Aust.* **4**, 451.
- Braz, M. A., and Scalise, E. (1982). *Astron. Astrophys.* **107**, 272.
- Caswell, J. L., Murray, J. D., Roger, R. S., Cole, D. J., and Cooke, D. J. (1975). *Astron. Astrophys.* **45**, 239.
- Caswell, J. L., Haynes, R. F., and Goss, W. M. (1977). *Mon. Not. R. Astron. Soc.* **181**, 427.
- Caswell, J. L., Batchelor, R. A., Forster, J. R., and Wellington, K. J. (1983*a*). *Aust. J. Phys.* **36**, 401.
- Caswell, J. L., Batchelor, R. A., Forster, J. R., and Wellington, K. J. (1983*b*). *Aust. J. Phys.* **36**, 443.
- Caswell, J. L., and Haynes, R. F. (1987*a*). *Aust. J. Phys.* **40**, 215.
- Caswell, J. L., and Haynes, R. F. (1987*b*). *Astron. Astrophys.* **171**, 261.
- Cohen, R. J., Baart, E. E., and Jonas, J. L. (1988). *Mon. Not. R. Astron. Soc.* **231**, 205.
- Forster, J. R., and Caswell, J. L. (1987). In 'Star Forming Regions', Proc. IAU Symp. No. 115 (Eds M. Peimbert and J. Jugaku), pp. 174-5 (Reidel: Dordrecht).
- Forster, J. R., and Caswell, J. L. (1989). *Astron. Astrophys.* (in press).
- Goss, W. M., Haynes, R. F., Knowles, S. H., Batchelor, R. A., and Wellington, K. J. (1977). *Mon. Not. R. Astron. Soc.* **180**, 51p.
- Kaufmann, P., Zisk, S., Scalise, E., Schaal, R. E., and Gammon, R. H. (1977). *Astron. J.* **82**, 577.
- Kemball, A. J., Gaylard, M. J., and Nicolson, G. D. (1988). *Astrophys. J. Lett.* **331**, L37.
- Kylafis, N. D., and Norman, C. A. (1989). *Astrophys. J.* (submitted).

- McCutcheon, W. H., Wellington, K. J., Norris, R. P., Caswell, J. L., Kesteven, M. J., Reynolds, J. E., and Peng, R.-S. (1988). *Astrophys. J. Lett.* **333**, L79.
- Norris, R. P., McCutcheon, W. H., Caswell, J. L., Wellington, K. J., Reynolds, J. E., Peng, R.-S., and Kesteven, M. J. (1988). *Nature* **335**, 149.
- Rodriguez, L. F., Moran, J. M., Ho, P. T. P., and Gottlieb, E. W. (1980). *Astrophys. J.* **235**, 845.
- Scalise, E., and Braz, M. A. (1980). *Astron. Astrophys.* **85**, 149.

Manuscript received 14 November 1988, accepted 20 January 1989